Microbuckling Failure of Circular Fiber-Reinforced Composites

L. B. Greszczuk*
McDonnell Douglas Astronautics Company, Huntington Beach, Calif.

Theoretical and experimental studies are presented on microbuckling compression failure of fiber-reinforced unidirectional composites subjected to compression loads parallel to the fiber direction. The approximate microbuckling equation is derived by the energy method. Results predicted from this equation are compared with test data and good agreement is found, indicating that for certain combinations of constituents, microbuckling is a valid failure mode. The influence of the following parameters on microbuckling is investigated theoretically and experimentally: fiber volume fraction, fiber shape, fiber size, properties of fibers and resins, fiber-end configuration, and specimen geometry. Other failure modes for composites subjected to compression loading are also briefly discussed.

Nomenclature

v = transverse displacement (in.)
ΔV = change in strain energy (lb/in.)
I = moment of inertia (in.^{4})
ℓ = buckle wavelength or specimen length (in.)
r = fiber radius (in.)
h = fiber diameter (in.)
$2c$ = fiber spacing (in.)
m = number of buckle waves
k = reinforcement volume fraction
E_f = Young's modulus of reinforcement (psi)
E_r = Young's modulus of resin (psi)
G_r = shear modulus of resin (psi)
G_{LT} = shear modulus of composite (psi)
τ = shear stress (psi)
γ = shear strain (in./in.)
γ_{LT} = shear strain in composite (in./in.)
P = compressive load (lb)
σ = compressive stress (psi)
x,y,z = orthogonal coordinates
n,a_n = terms in a series, Eq. (2)

Subscripts

c = composite
r = resin
f = reinforcement
S = shear mode

Introduction

A NUMBER of papers have been devoted to studying microbuckling as a possible failure mechanism for multilayered, or multilaminae, continua and unidirectional composites subjected to compressive loading in the direction of fibers or laminae. The problem of internal stability of single and multilayered media subjected to compressive loading has been investigated extensively by Biot in numerous papers and in his book.[1] For fiber-reinforced composites subjected to compressive loading, fiber microbuckling as a failure mode was apparently first suggested by Dow.[2] Using Timoshenko's column on the elastic foundation approach,[3] Rosen obtained equations for predicting the external loads at which fiber microbuckling takes place.[4] His mathematical model was two-dimensional, whereby the fibers and the matrix were idealized as laminae. The two possible buckling patterns for which equations were derived were the extension mode and the shear mode (Fig. 1). Solutions to microbuckling of lamina-reinforced composties have also been obtained by Schuerch,[5] Hayashi[6-8] Chung and Testa,[9] Greszczuk,[10] and others. In addition to considering the elastic microbuckling, Schuerch and Hayashi considered the inelastic microbuckling. A review of the theroetical work on the problem is presented by Greszczuk[10,11] whereas in Ref. 12 Greszczuk presents experimental results for laminae-reinforced composites to verify the two-dimensional microbuckling theory.

The problem of microbuckling compression failure of fiber-reinforced composites (three-dimensional problem) has been considered by Sadowsky, Pu, and Hussain,[13] Herrmann, Mason, and Chan,[14,15] and Greszczuk.[16] The solutions given by Sadowsky, et al.[13] and Herrmann, et al.[14,15] are for a problem of microbuckling of single round fiber surrounded and bonded by matrix material of infinite extent. An approximate solution to the microbuckling problem of multifiber reinforced composites was obtained by Greszczuk.[16] The latter solution and the experimental verification of the results are the subject of this paper.

Theoretical Considerations

As was the case with lamina-reinforced composites, when a circular fiber-reinforced composite is subjected to compressive loading parallel to the fiber direction, two types of microbuckling failures can take place: microbuckling in the extension mode and microbuckling in the shear mode. the two failure modes are illustrated in Fig. 1. In general, microbuckling in the extension mode will take place if the composite contains low volume fraction of the reinforcement ($k \leq 0.10$), whereas microbuckling in the shear mode will take place when $k \geq 0.10$.[4,5,9,11,12] Since the fiber volume fractions in actual composites are usually greater than ~ 0.10, only microbuckling in the shear mode is of interest and will be considered here. An approximate solution for the latter problem can be obtained by using the energy method.

As a composite changes from the compressed but unbuckled configuration to the buckled state, the change in strain energy of the fiber ΔV_f and the matrix ΔV_r has to be equal to the work done ΔT by the compressive forces P.

$$\Delta V_f + \Delta V_r = \Delta T \tag{1}$$

Assuming that the fibers buckle in phase with one another in a sinusoidal pattern expressed by the following series in v,

Presented as Paper 74-352 at the AIAA/ASME/SAE 15th Structures, Structural Dynamics and Materials Conference, Las Vegas, Nevada, April 17-19, 1974; submitted May 28, 1974; revision received March 3, 1975. The work described herein was sponsored by the Air Force Materials Laboratory, Air Force Systems Command, United States Air Force, Wright-Patterson AFB, Ohio, under Contract F33615-71-C-1399.

Index categories: Materials, Properties of; Structural Composite Materials (including Coatings).

*Principal Engineer/Scientist, Advance Structures and Mechanical Department. Member AIAA.

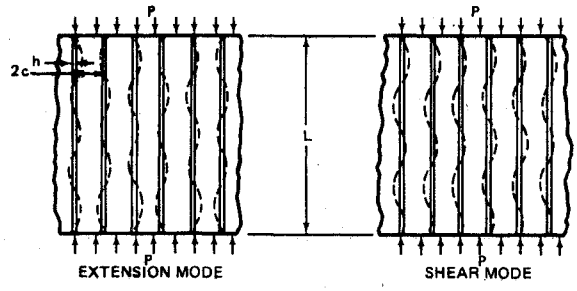

Fig. 1 Possible buckling patterns for unidirectional composites.

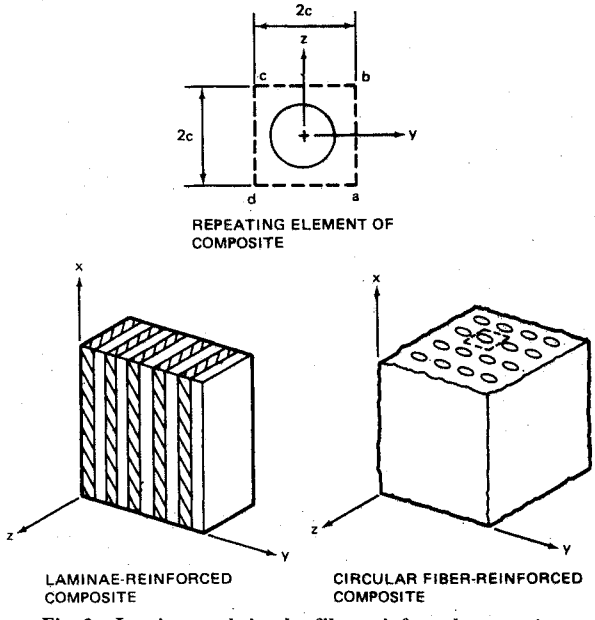

Fig. 2 Laminae and circular fiber-reinforced composites.

the displacement in the transverse direction,

$$v=\sum_{n=1}^{n=\infty} a_n \sin\frac{n\pi x}{\ell} \tag{2}$$

the strain energy of bending of the fiber is

$$\Delta V_f=\frac{E_f I}{2}\int_0^{\ell}\left(\frac{\mathrm{d}^2 v}{\mathrm{d}x^2}\right)^2 \mathrm{d}x=\frac{\pi^4 E_f I}{4\ell^3}\sum_{n=1}^{n=\infty} n^4 a_n^2 \tag{3}$$

The work done by the compressive force P acting on a fiber is[3]

$$\Delta T=\frac{P\pi^2}{4\ell}\sum_{n=1}^{n=\infty} n^2 a_n^2 \tag{4}$$

Assuming that the fiber shear deformation is negligible as compared to matrix shear deformation and neglecting the changes in strain energy associated with extensional stresses in the matrix, the change in strain energy for the matrix is

$$\Delta V_r=\tfrac{1}{2}\int_V \tau_{xyr}\,\gamma_{xyr}\,\mathrm{d}V \tag{5}$$

where the integration extends over a repeating volumetric element of composite. The task now is to relate the shear stress τ_{xyr} and shear strain γ_{xyr} in the matrix to the deformation of composite and its microstructure. In contrast to laminae-reinforced composites (Fig. 2) where γ_{xyr} are assumed to vary only in x-direction, that is,

$$\tau_{xyr},\ \gamma_{xyr}=f(x)\ldots \tag{6}$$

in the case of circular fiber reinforced composites these quantities are assumed to vary in x and z directions

$$\tau_{xyr},\ \gamma_{xyr}=f(x,\ z)\ldots \tag{7}$$

If a composite is subjected to an externally applied axial loading, conditions of symmetry require that the lines *ab*, *bc*, *cd*, and *da* (Fig. 2) in a deformed repeating element remain parallel to the corresponding lines in the undeformed material. In view of the assumption preceding Eq. (5), the following relationship can readily be established between the displacement of the fiber and shear strain the matrix[4] at any point z on the boundary of the repeating element

$$\gamma_{xyr}\approx(1/1-k_z)\ (\mathrm{d}v/\mathrm{d}x) \tag{8}$$

where

$$k_z=\left[\frac{4k}{\pi}-\left(\frac{z}{c}\right)^2\right]^{1/2} \tag{9}$$

k is the fiber volume fraction of a composite, z is a variable, and c is defined in Fig. 2. Equations (8) and (9) apply to composites containing a square array of circular fibers. For a given shear strain in the matrix, the shear stress is

$$\tau_{xyr}=G_r\,\gamma_{xyr} \tag{10}$$

and Eq. (5) becomes

$$\Delta V_r=\frac{G_r}{2}\int_V\left(\frac{\mathrm{d}v/\mathrm{d}x}{1-k_z}\right)^2\mathrm{d}V \tag{11}$$

which, after substitution for $\mathrm{d}v/\mathrm{d}x$ and integration of the resultant equation over the wavelength ℓ, yields

$$\Delta V_r=\frac{cG_r\pi^2}{2\ell}\sum_{n=1}^{n=\infty} n^2 a_n^2\int_{-c}^{c}\frac{\mathrm{d}z}{(1-k_z)} \tag{12}$$

Combining Eqs. (1, 3, 5, and 12) and solving for P yields

$$P=\left[2cG_r\sum_{n=1}^{n=\infty} n^2 a_n^2\int_{-c}^{c}\frac{\mathrm{d}z}{(1-k_z)}+\frac{\pi^2 E_f I}{\ell^2}\sum_{n=1}^{n=\infty} n^4 a_n^2\right]\Big/\sum_{n=1}^{n=\infty} n^2 a_n^2 \tag{13}$$

To determine the critical value of the load P we can proceed as described in Ref. 3 and obtain the following expression

$$P_{cr}=2cG_r\int_{-c}^{c}\frac{\mathrm{d}z}{(1-k_z)}+\frac{\pi^2 E_f I}{\ell^2}m^2 \tag{14}$$

where m is the number of buckle waves corresponding to P_{cr}. The critical compressive fiber stress is

$$(\sigma_f)_{cr}=\frac{2cG_r}{\pi r^2}\int_{-c}^{c}\left(\frac{\mathrm{d}z}{1-k_z}\right)+\frac{\pi^2 E_f}{4}\left(\frac{rm}{\ell}\right)^2 \tag{15}$$

in which, for square fiber packing,

$$c=r(\pi/4k)^{1/2} \tag{16}$$

and ℓ/m represents the buckle wavelength.

It has been shown in Ref. 15 that

$$G_{LT} = \frac{1}{2c} \int_{-c}^{c} \left(\frac{G_r}{1-k_z} \right) dz \tag{17}$$

where G_{LT} is the shear modulus of a circular fiber-reinforced composite.

Combining Eqs. (15-17), minimizing with respect to m, making use of relationship $(\sigma_f)_{cr} k = (\sigma_c)_{cr}$, the final equation for microbuckling stress of a composite having fibers with simply supported ends becomes

$$(\sigma_c)_{cr} = G_{LT} + (\pi^2 E_f k/4)\ (r/\ell)^2 \tag{18}$$

If the fibers have fixed ends, the following equation applies[16]:

$$(\sigma_c)_{cr} = G_{LT} + \pi^2\ E_f k (r/\ell)^2 \tag{19}$$

To verify the validity and the limitations of the microbuckling theory, extensive experimental studies have been conducted on nearly perfect fiber-reinforced model composites, the results of which are presented in the sections that follow.

Experimental Studies on Microbuckling Failure of Fiber-Reinforced Composite Models

The influence of the following parameters on the compressive microbuckling strength of fiber-reinforced composite models was investigated experimentally: fiber end fixity, fiber volume fraction, fiber array, specimen geometry, fiber diameter, and fiber and matrix properties. The various reinforcing materials and resin materials used in preparation of the specimens are described in Tables 1 and 2.

The composite models were fabricated in aluminum molds. The molds consisted of an elongated cavity of square cross section in a block of aluminum. Both ends of the cavity were closed with perforated aluminum plates. These perforated plates were provided with the array, spacing, and size of holes to give composites of various fiber volume fractions and various fiber arrays, and to accommodate various size fibers. To fabricate the composite models, the fibers were sand blasted, cleaned with acetone, inserted in the mold, and held in position by the end plates. Resin was then infiltrated between the fibers, and the assembly was cured. Each time a composite model was fabricated, a resin casting was made from the same resin batch as the composite. The resin casting was cocured with the composite, and tested for mechanical properties within ±3 hours from the time when the corresponding composites were tested.

Table 1 Average properties of reinforcing materials (measured)

Reinforcement	Compressive strength $\times 10^{-3}$ psi	Young's modulus in compression $\times 10^{-6}$ psi
Aluminum rods (6061-T6)	50.0	10.6
Stainless steel rods	266.2	27.4

Table 2 Average properties of resins (measured)

Resin	Young's modulus in compression (ksi)	Poisson's ratio	Remarks
A	2.5	0.470	
B	21.9	0.454	
C	61.9	0.445	
D	105.0	...	Highly nonlinear $\sigma-\epsilon$ curve
E	178.0	...	
F	457.0	0.41	

The dimensions of the test specimens were selected so that the specimens would fail by microbuckling rather than by Euler column buckling. For the composites that were tested, the relationship between the critical Euler buckling stress, $(\sigma_\epsilon)_{cr}$, and the critical microbuckling stress, $(\sigma_s)_{cr}$, for microbuckling in the shear mode† is[16]

$$(\sigma_\epsilon)_{cr} = \left[\frac{(t/r)^2}{(12 G_{LT}/\pi^2 E_f k)\ (\ell/r)^2 + 3} \right] (\sigma_s)_{cr} \tag{20}$$

where r is the fiber radius, t is the width or thickness of the composite specimen, G_{LT} is the shear modulus of composite, E_f is the Young's modulus of the fiber, k is the fiber volume fraction, and ℓ is the length of the specimen. For a typical composite that was tested ($E_f = 10.6 \times 10^6$ psi, $k = 0.50$, $t = 0.44$ in., $r = 0.039$ in., $\ell = 2.5$ in, $G_{LT} \approx 2.25\ G_r$, $G_r = 818$ psi) Eqs. (20) gives

$$(\sigma_\epsilon)_{cr} = 24.8\ (\sigma_s)_{cr}$$

Influence of Fiber-End Restraint

To establish the influence of the fiber-end restraint, experimental studies were conducted on fiber‡-reinforced composite models made with fibers having the following end configurations: flat ends, pyramid-shaped ends, and rounded ends. Figures 3 and 5 show specimens with fiber ends of various shapes. The reinforcement material in these models consisted of 6061-T6 aluminum rods arranged in square array, while the matrix was Resin A. The fiber diameter of composites shown in Fig. 3 was 0.125 in. while those shown in Fig. 4 were made with 0.125-in. and 0.078 in. diam fibers.

The composites were tested in compression in an Instron test machine, at a head speed rate of 0.05 in./min. Reference 16 contains the test results and complete descriptions of the test specimens, and shows the typical failures of the various specimens. The composites failed in one buckle wave as predicted by Eq. (15). In all cases the direction of buckle wave was approximately across the diagonal of the specimen's cross-section. The comparison of experimental results with theoretical results predicted by the microbuckling theory for circular fiber-reinforced composites, Eqs. (18) and (19), is shown in Fig. 5.

The latter shows that: 1) configuration of fiber ends has a significant influence on compressive buckling strength of composite models that were tested, and 2) theory for microbuckling of circular fiber-reinforced composites agrees quite well with the experimental data.

Influence of Fiber Volume Fraction

The volume fractions of composites that were fabricated and tested in compression ranged from $k = 3.3\%$ to $k = 64.6\%$. Figure 6 shows several composite specimens. All the composite specimens contained flat-ended fibers. Typical load-deflection curves for specimens containing various amounts of reinforcing material are shown in Fig. 7. When the critical microbuckling load was reached there was sudden drop in load.

The comparison of experimental results with the theoretical prediction, Eq. (19) is presented in Fig. 8. The theoretical curve was calculated using the average specimen geometry as well as average of all the properties of constituents corresponding to all the specimens for which test data are shown in Fig. 8.

The fact that the specimens described here failed by microbuckling follows similar reasoning to that presented in

†Assuming simply supported ends in both cases.

‡The terms fibers, rods, and reinforcement are used here interchangeably.

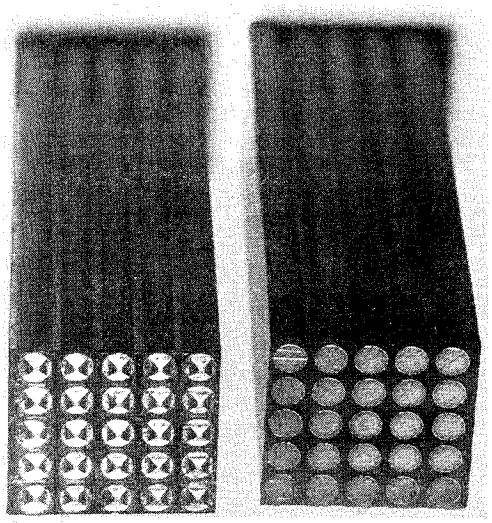

Fig. 3 Composite test specimens made with circular fibers having flat and pyramid shaped ends.

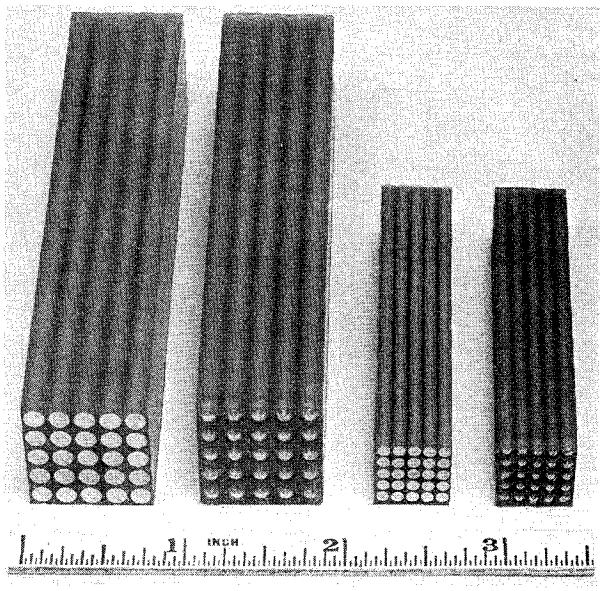

Fig. 4 Composite test specimens made with circular fibers having flat and rounded ends.

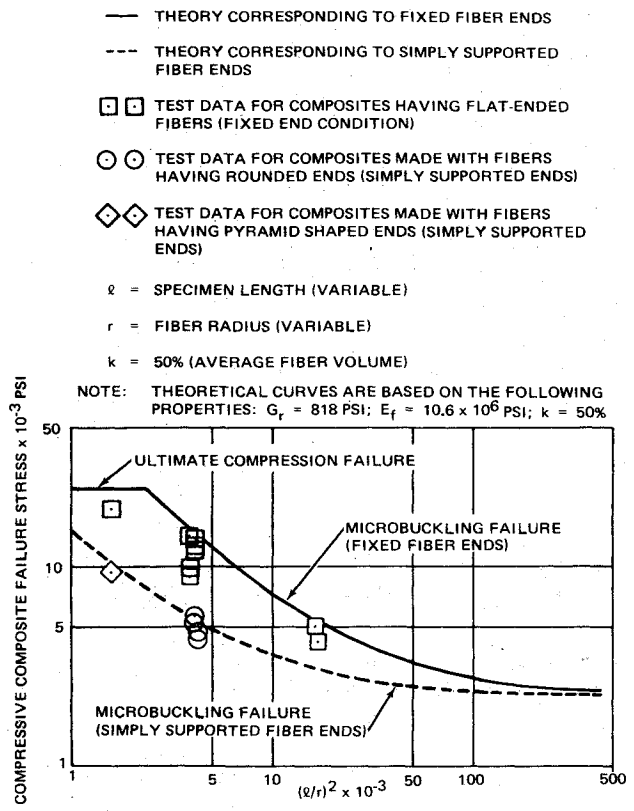

Fig. 5 Test theory comparison of compressive strength of composites made with aluminum fibers having various fiber-end configurations.

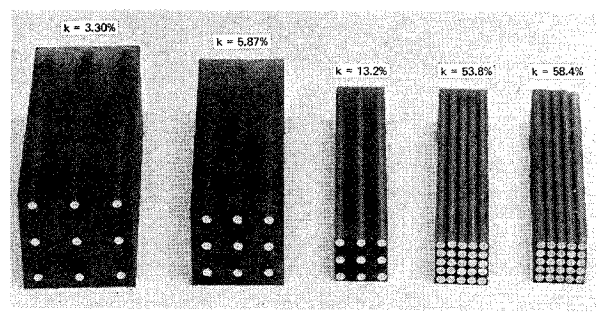

Fig. 6 Circular fiber-reinforced composite test specimens with different reinforcement volume fractions.

Refs. 11 and 16. Comparing the test data with theory based on the assumption that the fibers fail by microbuckling, and finding good correlation between the two, leads to a conclusion that fiber microbuckling is the failure mode.

Since the fiber-to-matrix modulus ratio of the specimens for which data are shown in Fig. 8 was $E_f/E_r \approx 4{,}000$ and the reinforcement volume fractions ranged from $k \approx 3.3\%$ to $k \approx 64.6\%$, all of the specimens failed in the shear mode as predicted by Eq. (15) which gives critical value of σ_f when $m = 1$. The comments made here regarding the failure modes of circular fiber-reinforced composites apply also to the results presented in the sections that follow.

Influence of Fiber Array

Composites with three different fiber arrays were investigated experimentally; square, hexagonal, and arbitrary. As before, the composites consisted of Resin A reinforced with 0.078-in. diam aluminum rods in the amount of approximately 50 volume %. Except for fiber array, all parameters remained constant. Figure 9 shows the three types of composite test specimens, while the typical load deflection curves for composites with different fiber arrays are shown in Fig. 10. Table 3 shows the test-theory comparison for compressive microbuckling strength of composites having various fiber arrays. The composite shear moduli used in these calculations were calculated from equations given in Ref. 17. From the results shown in Table 3, it is not obvious how fiber array influences the compressive microbuckling strength. This in part is because the geometry of composites that were tested was such that microbuckling was governed primarily by the second term in Eq. (19), which does not involve the shear modulus of the composite. By increasing the length of the specimen or the shear modulus of the matrix, the compressive microbuckling strength would be expected to be primarily a function of the shear modulus of the composite. Figure 11 shows the predicted composite microbuckling compressive strength as a function of shear modulus of the resin for composites with two different fiber arrays.

Influence of Fiber Size and Specimen Geometry

The influence of fiber size on compressive microbuckling strength of composites was studied using 25 rod composites

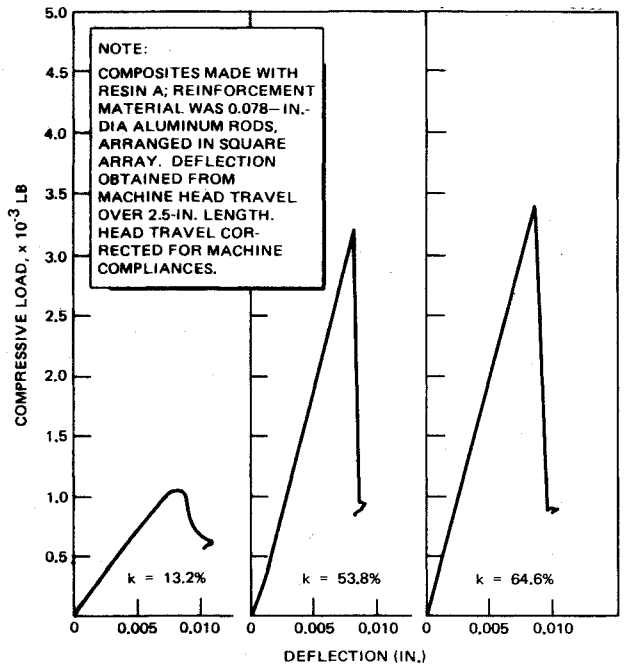

Fig. 7 Typical load-deflection curves for circular fiber-reinforced composites subjected to compressive loading.

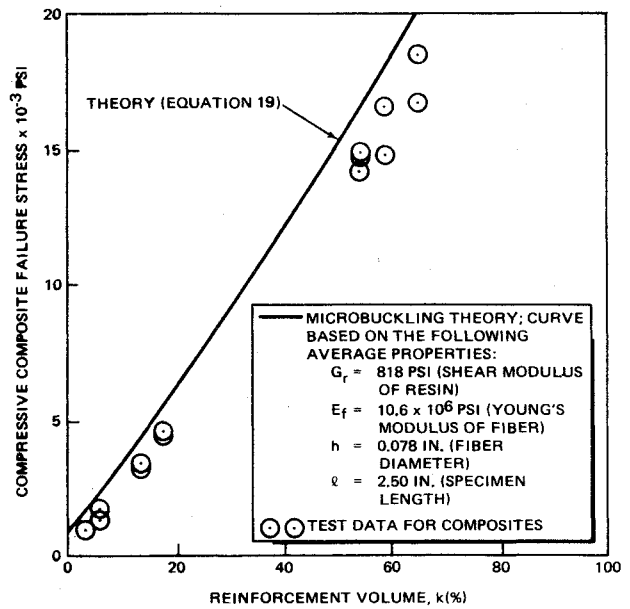

Fig. 8 Test-theory comparison of compressive micro-buckling strength of circular fiber-reinforced composites having various fiber volume fractions.

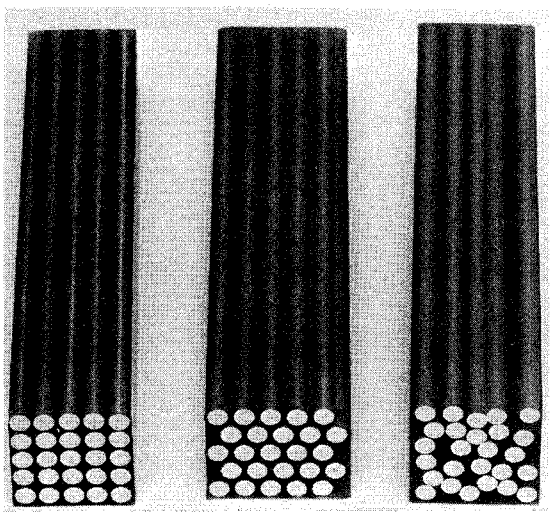

Fig. 9 Composite test specimens with square, hexagonal, and arbitrary fiber arrays.

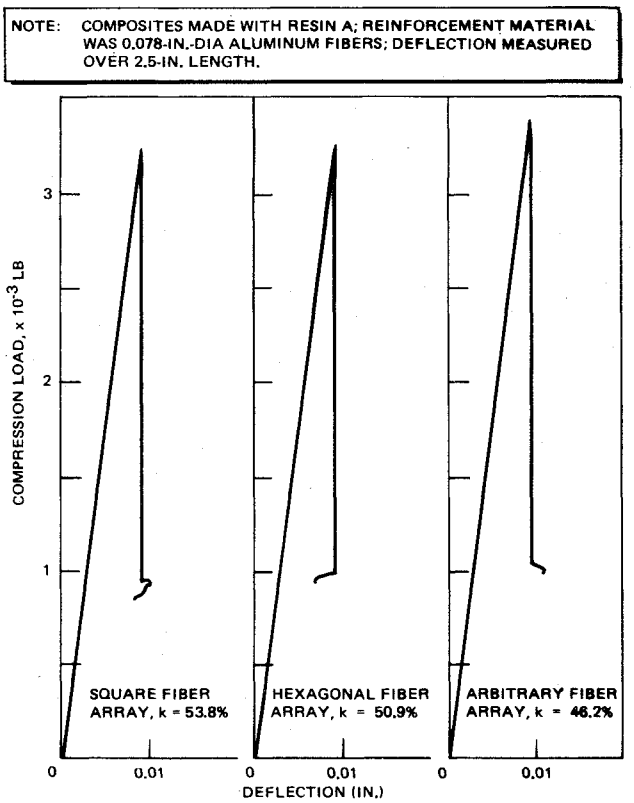

Fig. 10 Typical load-deflection curves for circular fiber-reinforced composites having various fiber arrays.

Table 3 Test-theory comparison of compressive microbuckling strength of composites having various fiber arrays

Fiber array	Fiber volume fraction	Resin shear modulus G_r (psi)	Composite failure stress (psi) Test	Theory	Test / Theory
Square	53.0	827	14,620	15,850	0.922
Square	52.6	816	14,320	15,660	0.915
Hexagonal	46.2	877	12,980	13,460	0.964
Hexagonal	46.2	849	12,560	13,402	0.936
Arbitrary	47.7	724	12,930	13,720	0.942
Arbitrary	48.5	776	13,920	14,092	0.988

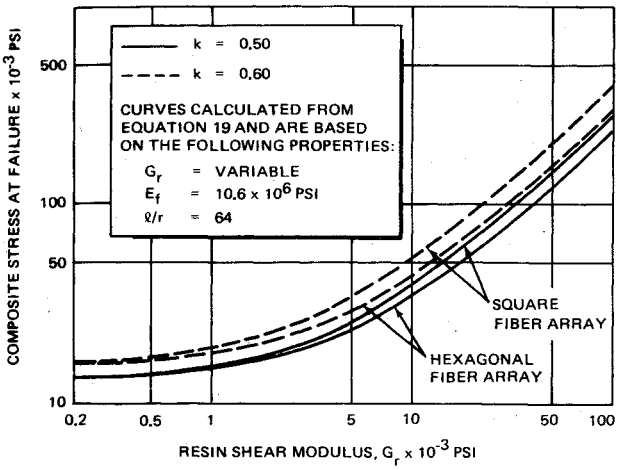

Fig. 11 Theoretical results on influence of resin shear modulus, fiber content, and fiber array on compressive microbuckling strength of composites.

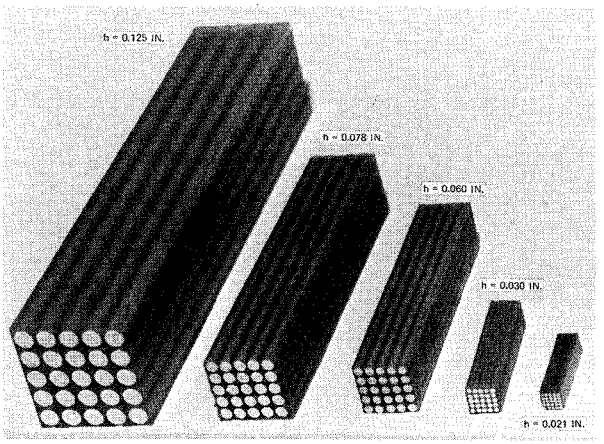

Fig. 12 Composite test specimens with various diameter fibers and reinforcement volume of 50%.

reinforced with 6061-T6 aluminum fibers of the following nominal diameters: 0.020, 0.030, 0.060, 0.078, and 0.125 in. All the rods of various diameters were machined on a centerless grinder from 0.125-in. diam rods. This was done to minimize any variations in material properties that could have existed if extruded rods of various diameters were employed. The composites were made with Resin A and contained approximately 50 % reinforcement by volume. The specimen length-to-fiber-diameter ratio was approximately the same for all the specimens.

Several of the test specimens are shown in Fig. 12, while typical load-deflection curves for composites made with various size fibers are shown in Fig. 13. Table 4 shows a comparison of experimental results with theoretical results predicted from Eq. (19).

Since all composites had approximately a constant (ℓ/r) and contained approximately the same amount of reinforcing material, they should have had approximately the same compressive strength, as predicted by Eq. (19). As shown in Table 4, this is not true; there appears to be fiber size effect. Except for composites made with 0.125-in. diam rods, the compressive strength is shown to decrease as the fiber diameter decreases. One possible reason for compressive strength decrease of composites with decreasing fiber diameter is the influence of initial imperfections. As the fiber diameter decreases, the fibers become more flexible and are more likely to possess imperfections such as slight curvature. These imperfections could have been introduced during grinding of rods, during preparation of composite specimens, or during

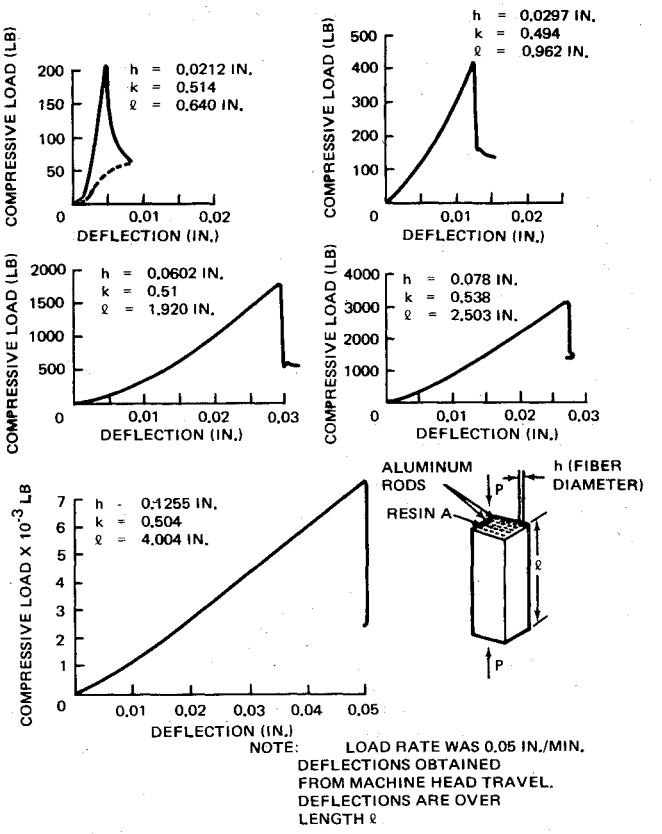

Fig. 13 Load-deflection curves for composites made with fibers of various diameters.

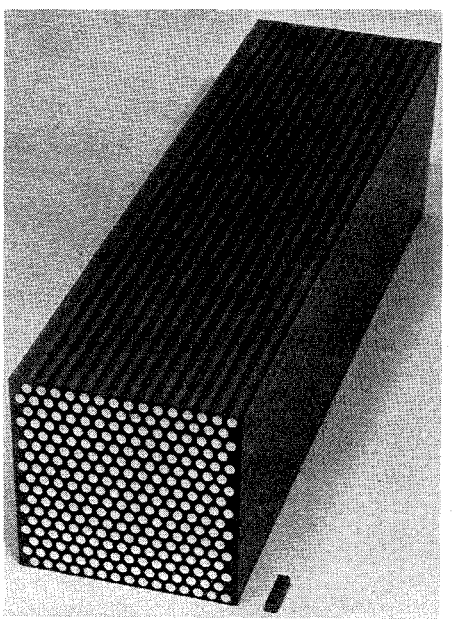

Fig. 14 Composite test specimens of various sizes.

curing of composites. As shown in Ref. 16, for a composite made with 0.0212-in. diam fibers, a fiber bow in the amount of 0.0015-in. arc height in 0.64-in. length would be sufficient to cause strength reductions shown in Table 4. As to the composites made with 0.125-in. diam rods, no explanation has yet been found for the sudden trend reversal in strength vs fiber diameter. The only thing different about the latter composites was that no machining was done on the 0.125-in. diam to various smaller diameters. Thus, there exists a possibility that the as-received 0.125-in. diam rods contained imperfections.

Table 4 Test-theory comparison of compressive microbuckling strength of composites with various size fibers

Fiber diam. (in.)	Fiber content (%)	Resin shear modulus (psi)	ℓ/r	Compressive strength (psi) Test	Theory	Test / Theory
0.0212	43.8	622	60.2	9,990	13,892	0.719
0.0212	43.5	622	60.3	10,260	13,825	0.741
0.0297	48.5	927	64.8	10,940	14,410	0.760
0.0297	46.7	927	64.8	11,330	13,800	0.822
0.0602	50.0	826	63.8	12,360	14,992	0.824
0.0602	51.1	877	63.8	13,260	15,520	0.854
0.0779	53.0	827	64.2	14,620	15,738	0.931
0.0779	52.6	816	64.2	14,320	15,658	0.916
0.0779	52.6	851	64.2	13,870	15,678	0.885
0.1255	50.4	767	63.7	13,000	14,965	0.869
0.1255	49.3	777	63.7	12,230	14,660	0.834
Average	49.3	804	63.4	...	...	...

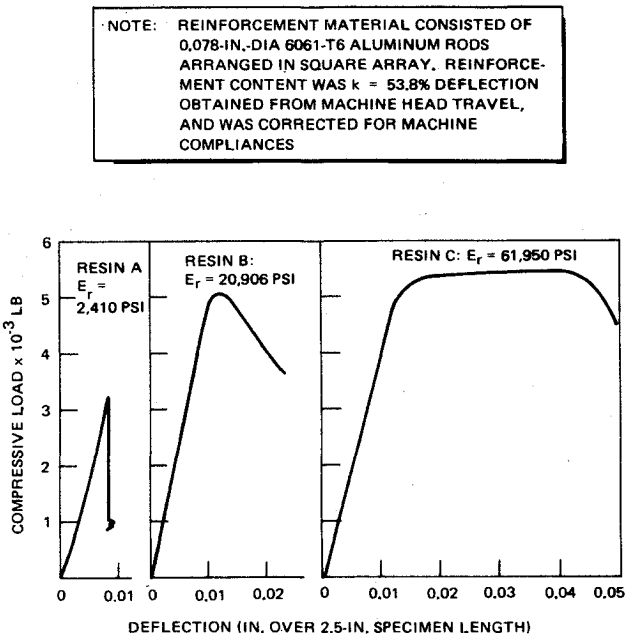

Fig. 15 Typical compressive load-deflection curves for aluminum rod-reinforced composites made with resins having different moduli of elasticity.

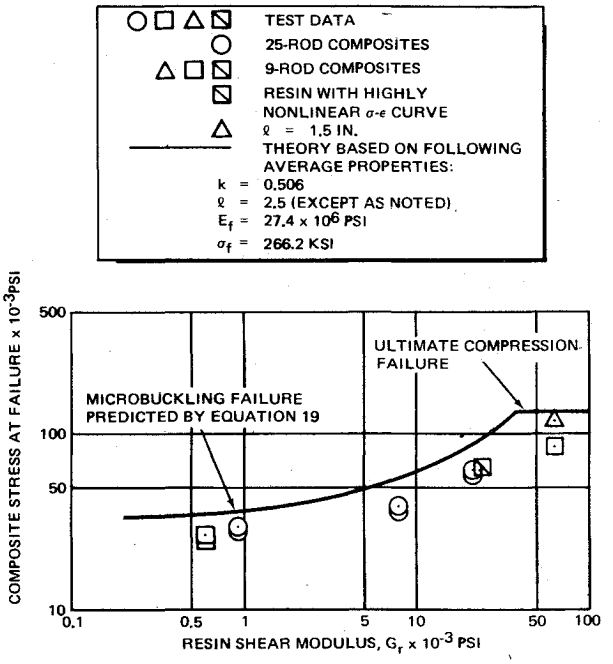

Fig. 16 Test-theory comparison of compressive strength of composites consisting of stainless steel rods and resins with different shear moduli.

In addition to the tests on composites of various dimensions made with fibers of various sizes, several composites were fabricated whereby the length and size of the composite was the test variable. The largest and the smallest of these composites are shown in Fig. 14.

Influence of Constituent Properties

The reinforcing materials and the matrix materials used in this investigation are described in Tables 1 and 2. Composite specimens were prepared from various combinations of constituents and were tested in compression as described previously. Most of the composites that were tested contained 25, 0.078-in. diam rods arranged in square array and contained appproximately 0.50 reinforcement material by volume. Moreover, all specimens tested were of approximately the same geometry. In the case of aluminum rod-reinforced composites, the influence of both the reinforcement content and the matrix properties on compressive failure of composites was investigated. In the case of stainless steel composites, matrix material was the only test variable. Figure 15 shows typical load-deflection curves for composites made with aluminum rods and three different resins. All composites made with Resin A failed by elastic microbuckling. Composites made with Resin B exhibited some nonlinearity in the load-deflection curve near the point of failure, indicating initiation of yielding of the reinforcement. Composites made with Resin C failed by compression yielding followed by inelastic buckling. Similar results were obtained for composites reinforced with stainless steel rods.[10,11] A comparison of experimental results obtained from specimens discussed in this section with theoretical results predicted by Eq. (19) is shown in Figs. 16 and 17.

Discussion and Conclusions

From the experimental results presented in the previous section, it is obvious that for composites made with low modulus resin, microbuckling is the critical failure mode. As the Young's and shear moduli of the resin are increased, the mode of failure changes to nonmicrobuckling compression failure of the reinforcement (Fig. 17). The nonmicrobuckling compressive failure stress can be obtained from the following ap-

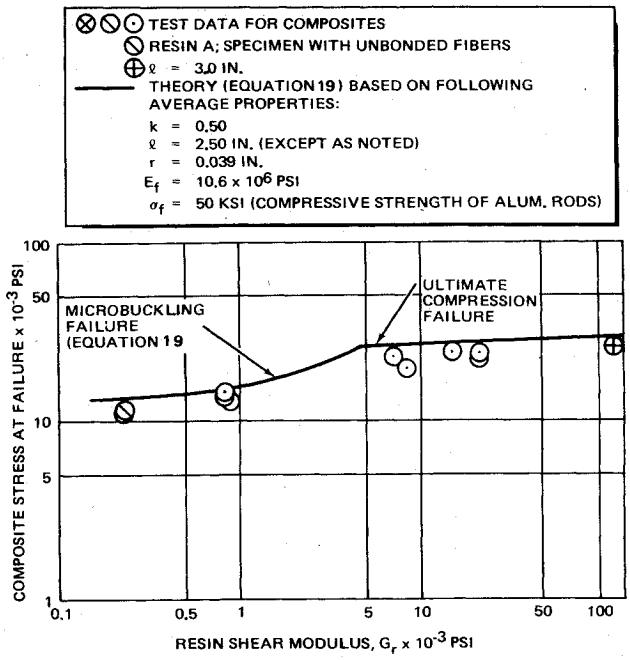

Fig. 17 Test-theory comparison of compressive strength of composites made with aluminum rods as influenced by shear modulus of resin.

proximate equation

$$\sigma_c \approx \sigma_f k + \sigma_r (1-k) \tag{21}$$

where σ_f is the compressive strength of the reinforcement, k is its volume fraction, and σ_r is the compressive stress in the matrix corresponding to a strain $\epsilon_r = \sigma_f / E_f$.

For actual composites such as graphite/epoxy and boron/epoxy the specimen length ℓ is generally much greater than the fiber radius r and therefore the equation for predicting microbuckling compression failure Eqs. (18 or 19) reduces to

$$(\sigma_c)_{cr} = G_{LT} \tag{22}$$

Application of the previous equation to actual composites shows that the room temperature compressive strength of such composites predicted from Eqs.(22) is much greater than the measured values. Recent studies on the failure modes in actual composites[16] show that such composites can fail in another mode: by transverse tensile failure or fiber-matrix debonding prior to microbuckling. This failure mode results from transverse tensile stresses (normal to the direction of the fibers) which are induced in a composite subjected to compression loading in the fiber direction as a result of the differences between the Poisson ratio of the fibers and the matrix. For the latter case the final failure can still be by microbuckling, however, the compression load at which microbuckling takes place will be governed by the shear modulus of a composite with unbonded or partially bonded fibers, G^*_{LT}, rather than by shear modulus G_{LT} which was calculated assuming perfect fiber-matrix bond up to failure. The analysis of microbuckling failure of composites with partially bonded or unbonded fibers is outside the scope of this paper, however, some approximate results of influence of unbonded fibers are presented in Ref. 18.

Another factor which influences the loads at which microbuckling failure takes place is the inelastic and nonlinear behavior of the fibers and the matrix. Although the nonlinear effects in fibers used in structural composites are expected to be small, the nonlinear behavior of the matrix is expected to significantly affect the loads at which microbuckling takes place. As in the case with more conventional buckling problems, prebuckling fiber deformations within the composite have also a significant influence on the loads at which microbuckling failures take place.[16] Such deformations are incurred during fabrication of composites, or as a result of using twisted yarns or because of fiber misalignment.

References

[1] Biot, M. A., *Mechanics of Incremental Deformation*, Wiley, New York, 1965, pp. 227-259.

[2] Dow, N. F. and Gruntfest, I. J., "Determination of Most Needed Potentially Possible Improvements in Materials for Ballistic and Space Vehicles," TIS R60SD389, June 1960, General Electric Co., Space Sciences Lab., Valley Forge, Pa.

[3] Timoshenko, S. P. and Gere, J. M., *Theory of Elastic Stability*, McGraw-Hill, N.Y., 1936.

[4] Rosen, B. W., *Fiber Composite Materials*, American Society for Metals, Metals Park, Ohio, 1965, Chapt. 3.

[5] Schuerch, H., "Prediction of Compressive Strength in Uniaxial Boron Fiber-Metal Matrix Composite Materials," *AIAA Journal*, Vol. 4, Jan. 1966, pp. 102-106.

[6] Hayashi, T., *Proceedings of the 7th British Plastics Federation (International Reinforced Plastics) Conference*, Brighton, England, Oct. 1970.

[7] Hayashi, T., "On the Shear Instability of Structures Caused by Compressive Loads," AIAA Paper 65-770, Los Angeles, Calif., Nov. 1965.

[8] Hayashi, T., "On the Shear Instability of Structures Caused by Compressive Loads," *Proceedings of the 16th Japan National Congress for Applied Mechanics*, 1966, pp. 149-157.

[9] Chung, Wen-Yi and Testa, R. B., "The Elastic Stability of Fibers in a Composite Plate," *Journal of Composite Materials*, Vol. 3, Jan. 1969, pp. 58-80.

[10] Greszczuk, L. B., "Compressive Strength and Failure Modes of Unidirectional Composites," in *Analysis of the Test Methods for High-Modulus Fibers and Composites*, ASTM STP 521, 1973, American Society for Testing Materials, Philadelphia, Pa.

[11] Greszczuk, L. B., "Microbuckling of Unidirectional Composites," Final Rept. Contracts F33615-67-C-1559 (Projects 2414 and 2731) and F33615-69-C-1001 (Project 2731), March 1971, Air Force Materials Lab., Wright-Patterson Air Force Base, Ohio.

[12] Greszczuk, L. B., "Microbuckling of Lamina-Reinforced Composites," *Presented to American Society for Testing and Materials Conference*, Williamsburg, Va, March 1973.

[13] Sadowsky, M. A., Pu, S. L., and Hussain, M. A., "Buckling of Microfibers," *Journal of Applied Mechanics*, Vol. 34, Ser. C, Dec. 1967, pp. 1011-1016.

[14] Herrmann, L. R., Mason, W. E., and Chan, S. T. K., "Response of Reinforcing Wires to Compressive States of Stress," *Journal of Composite Materials*, Vol. 1, July 1967, pp. 212-226.

[15] Herrmann, L. R., Mason, W. E., and Chan, S. T. K., "Behavior of Compressively Loaded Reinforcing Wires," *Structural Engineering Laboratory Rept. 67-2*, Jan. 1967, University of California, Berkeley, Calif.

[16] Greszczuk, L. B., "Failure Mechanics of Composites Subjected to Compressive Loading," AFML-TR-72-107, Air Force Materials Lab., Wright-Patterson Air Force Base, Ohio.

[17] Greszczuk, L. B., "Interfiber Stresses in Filamentary Composites," *AIAA Journal*, Vol. 9, July 1971, pp. 1274-1280.

[18] Greszczuk, L. B., "Consideration of Failure Modes in the Design of Composite Structures," *Presented to NATO AGARD Meeting*, Munich, Germany, Oct. 1974.